Estimation of the degree of dynamical instability from the information entropy of symbolic dynamics

Takaya Miyano*
Department of Mechanical Engineering, Ritsumeikan University, 1-1-1 Noji-higashi, Kusatsu, Shiga 525-8577, Japan

Hiroshi Gotoda†
Department of Mechanical Engineering, Tokyo University of Science, 6-3-1 Niijuku, Katsushika-ku, Tokyo 125-8585, Japan
(Received 28 June 2017; revised manuscript received 4 September 2017; published 9 October 2017)

A positive Lyapunov exponent is the most convincing signature of chaos. However, existing methods for estimating the Lyapunov exponent from a time series often give unreliable estimates because they trace the time evolution of the distance between a pair of initially neighboring trajectories in phase space. Here, we propose a mathematical method for estimating the degree of dynamical instability, as a surrogate for the Lyapunov exponent, without tracing initially neighboring trajectories on the basis of the information entropy from a symbolic time series. We apply the proposed method to numerical time series generated by well-known chaotic systems and experimental time series and verify its validity.

DOI: 10.1103/PhysRevE.96.042203

I. INTRODUCTION

In an isolated system at thermodynamical equilibrium, the thermodynamical entropy S associated with a thermal flow is equalized to the logarithmic number, $\log W$, of distinct microscopic states of the system via Boltzmann's equation $S = k_B \log W$ with Boltzmann's constant k_B. In nonlinear dynamical systems, which include nonconservative dissipative systems far from thermodynamical equilibrium, the Kolmogorov-Sinai (KS) entropy $h(\rho)$ representing the rate of creation of information with time on an attractor with a Lebesgue measure ρ is equalized to the sum of positive Lyapunov exponents $\lambda_i > 0\,(i = 1, \ldots, n)$ via Pesin's theorem expressed as $h(\rho) = \sum_{i=1}^{n} \lambda_i$ [1]. Under ergodicity, these theorems enable us to understand the dynamical nature of a dynamical system on the basis of its statistical properties.

Nonlinear time series analysis is an important tool for detecting chaos from sparse experimental data measured at finite sampling time intervals. Previous literature reported numerical algorithms to estimate the largest Lyapunov exponent from an experimental time series of a single variable; see for instance, the work of Sano and Sawada [2], Rosenstein *et al.* [3], and Kantz [4]. A positive Lyapunov exponent is the most convincing signature of chaos, which indicates an exponentially rapid divergence of infinitesimally nearby trajectories in phase space. However, these algorithms often yield unreliable estimates, particularly, for noisy time series. This is because they trace a pair of dynamically unstable trajectories containing observational noise, which blurs the initial rapid growth of a small distance between the trajectories. To circumvent this problem and develop an alternative method for estimating the degree of dynamical instability, we can resort to the statistical properties of an observed chaotic behavior such as the probability density function or the information entropy, instead of tracing a pair of chaotic trajectories. This is the motivation of this study.

The information entropy, originally introduced by Shannon [5], has been applied to time series analysis by many authors [6–15]. Fraser and Swinney applied mutual information to determine the optimal time lag for embedding from a time series of a single variable [6,7]. Costa *et al.* demonstrated a method for estimating a variant of the information entropy, referred to as multiscale entropy, from a sequence of mean values over segments of a time series to analyze the dynamical nature of the time series in terms of multiple time scales [8]. Bandt and Pompe introduced the permutation entropy [9,10]. In their method, a time series is transformed into a sequence of symbols expressed by permutations of data points in short segments of the time series, and the entropy is estimated from the probability density function approximated by the histogram of the symbols. They reported that such coarse-graining of a time series is effective for assessing the degree of complexity of the series. Amigó *et al.* discussed the relationship between the permutation entropy and the metric entropy rate [11]. The symbolic dynamics based on permutational coarse-graining have been shown to be effective for detecting chaos from experimental time series [12–15]. Politi also applied a modified version of the permutation entropy to estimate the KS entropy as well as the fractal dimension for numerical chaotic time series [16]. Recently, Weilenmann *et al.* discussed the axiomatic relationship between the thermodynamic and information entropies [17].

In this paper, we propose a method for estimating the degree of dynamical instability, as a surrogate for the largest Lyapunov exponent or the KS entropy, of a chaotic system from the information entropy of a sequence of symbols, referred to as "alphabets," transformed from a time series. In particular, unlike the method proposed in Ref. [16], we use the information entropy as a function of the sampling time interval of a time series. We apply three different methods based on permutation, global binarization, and local binarization to coarse-grain a time series into symbolic sequences. The alphabets comprising the symbolic sequence can be viewed as "microscopic states" that are occupied by the time series representing a macroscopic dynamical behavior of the chaotic system. As the sampling time interval increases, a chaotic time

*tmiyano@se.ritsumei.ac.jp
†gotoda@rs.tus.ac.jp

series has more opportunities to occupy different microscopic states, which should reflect the rapid growth of the distance between neighboring trajectories. We statistically estimate the rate of the initial growth of the information entropy, which may be linearly correlated with the largest Lyapunov exponent or the KS entropy, without directly measuring the distance between neighboring trajectories in phase space. The validity of this idea is examined in the following sections of this paper. Consequently, it turns out that there is a linear correlation between the initial growth rate of the entropy and the largest Lyapunov exponent, and the proportional constant between them may be unique and indicative of the equivalence of the growth rate to the KS entropy.

II. MATHEMATICAL METHOD

The methods we use to coarse-grain a time series into a symbolic sequence are as follows. Given a time series $\{x(t_0+nT)\}_{n=0}^{N-1}$ consisting of N data points (observations), where T denotes the sampling time interval of the time series and t_0 is the initial time of measurement (usually set to 0), we partition the time series into Q nonoverlapping segments each consisting of D contiguous data points so as to satisfy $N = QD$. An alphabet is assigned to each segment using the following procedures.

The first method is based on the permutation of D data points in each segment in the same way as that when estimating the permutation entropy [9,10]. We give an integer score to each data point in the segment in accordance with its rank order. The sequence of D rank scores represents the alphabet assigned to the segment. For example, when $D = 4$, there are $D! = 24$ patterns of the rank-score sequence and the corresponding 24 alphabets are defined as "1234," "1243," "1324," "1342," "1423," "1432," "2134," "2143," "2314," "2341," "2413," "2431," "3124," "3142," "3214," "3241," "3412," "3421," "4123," "4132," "4213," "4231," "4312," and "4321." This method cannot define the alphabets for a flat time series or a partly flat time series. Such cases can be encountered when handling experimental data observed with a low measurement resolution. It is also likely to misassign alphabets when a time series is contaminated with observational noise. Bian *et al.* developed a modified version of the permutation entropy, wherein rank-score sequences including equal rank scores, such as "1123" and "2221," are incorporated in the alphabets [18]. They showed that their method was effective for characterizing the complexity of time series for medical data of heart rate variability. However, owing to the increase in the total number of alphabets, their method requires a large number of data points to avoid a biased estimation of the permutation entropy.

The second method is based on the binary coding of a time series using global threshold crossing. In this method, we find a global threshold value x_c around which the time series is distributed with equal probability. The time series is transformed into a binary sequence $\{b(nT)\}_{n=0}^{N-1}$ consisting of values of 0 and 1 using $b(nT) = 0$ if $x(nT) < x_c$ and $b(nT) = 1$ otherwise. We define the alphabet of each segment using 2^D patterns of D binarized data points. For example, when $D = 4$, there are $2^D = 16$ alphabets expressed as "0000," "0001," "0010," "0011," "0100," "0101," "0110," "0111," "1000," "1001," "1010," "1011," "1100," "1101," "1110," and "1111." The threshold x_c can be easily found when the time series is distributed symmetrically around x_c. However, the probability distribution must be estimated to find x_c when the time series does not have a symmetrical distribution.

The third method is based on the binary coding of a time series using local threshold crossing. We estimate the mean over D data points of the ith segment, denoted as $\bar{x}_i$, with i running from 0 to $Q-1$ corresponding to Q segments:

$$\bar{x}_i = \frac{1}{D}\sum_{n=0}^{D-1} x[(iDT + nT)]. \tag{1}$$

The time series is locally binarized with the threshold crossing using $\bar{x}_i$ instead of x_c and the alphabet of each segment is defined in the same way as in the second method. The third method can be readily performed even if the data points are distributed asymmetrically. However, the alphabet "0000" is always missing and "1111" appears if and only if a segment is flat.

The first and third methods locally assign alphabets to the segments of a time series, whereas the second method globally assigns alphabets to them. Let us denote the assigned alphabets as a_i, with i running from 1 to $D!$ for the method based on permutation and from 1 to 2^D for the methods based on the global and local threshold crossings. The probability density function $p(a_i)$ of the alphabets is estimated from their histogram. Thus, the information entropy $H(T)$ as a function of the sampling time interval is estimated to be

$$H(T) = -\sum_{i=1}^{M} p(a_i)\log_2 p(a_i), \tag{2}$$

where M is the total number of the alphabets, i.e., $M = D!$ or $M = 2^D$. It is convenient to normalize $H(T)$ with respect to its maximum value $H_{\max}$, where $H_{\max} = \log_2(D!)$ bits for the alphabets generated by permutation and $H_{\max} = D$ bits for those generated by the global and local threshold crossings. Let us define the permutation entropy (PE) as $h(T) = H(T)/\log_2(D!)$ and the entropy based on the global and local threshold crossings, referred to as the string entropy with a global threshold (SEG) and the string entropy with local thresholds (SEL), respectively, as $h(T) = H(T)/D$. For all entropies, $0 \leqslant h(T) \leqslant 1$.

We next conduct the Taylor expansion of $h(T)$ as

$$h(T) = h(0) + h'(0)T + O(T^2) + \ldots, \tag{3}$$

$$\approx h(0) + \alpha T, \tag{4}$$

where h' represents the derivative of $h(T)$ with respective to time and $\alpha = h'(0)$ is a coefficient having the physical dimension of the inverse time similar to that of the Lyapunov exponent. When we observe a time series with a sampling time interval of $T \ll 1$, we may linearize $h(T)$ to obtain Eq. (4). In Eqs. (3) and (4), $h(0)$ should be interpreted to represent PE, SEG, and SEL in the limit of continuous measurement of a time series at $T \to 0$. In the limit with $D = 4$, only two alphabets, "1234" and "4321," appear in the case of PE, only "0000" and "1111" almost certainly appear in the case of SEG, and only "0011" and "1100" appear in the case of SEL. Hence,

TABLE I. Estimates of α and $h(0)$ calculated from PE, SEG, and SEL for time series of the variables x, y, and w for various chaotic flows in comparison with the largest Lyapunov exponent λ cited from Ref. [19]. The least-mean-square method was applied to $h(T)$ for the time series with $\Delta t \leqslant T \leqslant 5\Delta t$ to estimate α and $h(0)$. The correlation coefficient indicating the degree of fidelity in the linear fitting is denoted as γ.

Model and variable	Entropy	α	$h(0)$	γ	λ
Driven van der Pol, x	PE	1.7978	0.2261	0.9992	0.1933
	SEG ($x_c = 0$)	2.0554	0.2611	0.9987	
	SEL	1.9698	0.2586	0.9998	
Forced Brusselator, x	PE	0.9744	0.2175	0.9903	0.0140
	SEG ($x_c = 0.345$)	0.8768	0.2545	0.9976	
	SEL	0.9599	0.2547	0.9930	
Forced Brusselator, y	PE	0.4894	0.1947	0.9982	0.0140
	SEG ($y_c = 2.816$)	0.7705	0.2541	0.9990	
	SEL	0.5308	0.2235	0.9979	
Duffing's two-well, x	PE	0.9790	0.2231	0.9987	0.1572
	SEG ($x_c = 0$)	0.8446	0.2528	0.9996	
	SEL	1.0535	0.2559	0.9988	
Lorenz, x	PE	4.6344	0.2500	0.9986	0.9056
	SEG ($x_c = 0$)	2.5031	0.2663	0.9979	
	SEL	4.1382	0.2955	0.9952	
Lorenz, y	PE	6.6749	0.2644	0.9982	0.9056
	SEG ($y_c = 0$)	3.7457	0.2769	0.9989	
	SEL	5.8883	0.3143	0.9944	
Rössler, x	PE	1.1570	0.2231	0.9978	0.0714
	SEG ($x_c = 0$)	1.7571	0.2574	0.9996	
	SEL	1.2462	0.2560	0.9972	
Rössler, y	PE	1.2033	0.2221	0.9996	0.0714
	SEG ($y_c = 0$)	1.6556	0.2588	0.9977	
	SEL	1.3027	0.2548	0.9994	
Chua's circuit, x	PE	2.3384	0.2288	0.9990	0.3271
	SEG ($x_c = 0$)	1.1152	0.2547	0.9973	
	SEL	2.4591	0.2631	0.9982	
Chua's circuit, y	PE	2.5941	0.2317	0.9990	0.3271
	SEG ($y_c = 0$)	3.4551	0.2758	0.9971	
	SEL	2.6794	0.2671	0.9984	
Driven pendulum, y	PE	1.9822	0.2269	0.9982	0.1633
	SEG ($y_c = 0$)	0.7581	0.2508	0.9964	
	SEL	2.0769	0.2615	0.9977	
Hénon–Heiles, x	PE	1.2558	0.2171	0.9935	0.0450
	SEG ($x_c = 0$)	1.8525	0.2510	0.9978	
	SEL	0.9129	0.2596	0.8763	
Hénon–Heiles, w	PE	1.6396	0.2091	0.9802	0.0450
	SEG ($w_c = 0$)	1.9315	0.2513	0.9968	
	SEL	1.4812	0.2471	0.9244	

$h(0) = 1/\log_2(D!) \approx 0.2181$ for PE and $h(0) = 1/D = 0.25$ for SEG and SEL. Such tendencies should appear when D is set to an even integer. For SEL, however, there is inevitably ambiguity in defining the alphabets corresponding to $h(0)$ when D is set to an odd integer. For example, when $D = 5$, the alphabets appearing in the limit can be the pair of "00011" and "11100," or the pair of "00111" and "11000." This will be demonstrated through numerical experiments in the next section.

Since $h(T) \to h(0)$ as $T \to 0$ and $h(T) \to 1$ as $T \to \infty$, α is expected to take positive values for chaotic time series. Let us tentatively assume $h(T)$ to be a sigmoid function of T of the form

$$h(T) = \frac{h(0)}{h(0) + [1 - h(0)]e^{-\beta T}}, \tag{5}$$

$$\approx h(0) + \alpha T, \tag{6}$$

$$\alpha = \beta h(0)[1 - h(0)], \tag{7}$$

where β is assumed to be a real function f of the Lyapunov exponent λ: $\beta = f(\lambda)$. In the case of a single positive Lyapunov exponent, λ represents the largest Lyapunov exponent. In the case of multiple positive Lyapunov exponents, λ should

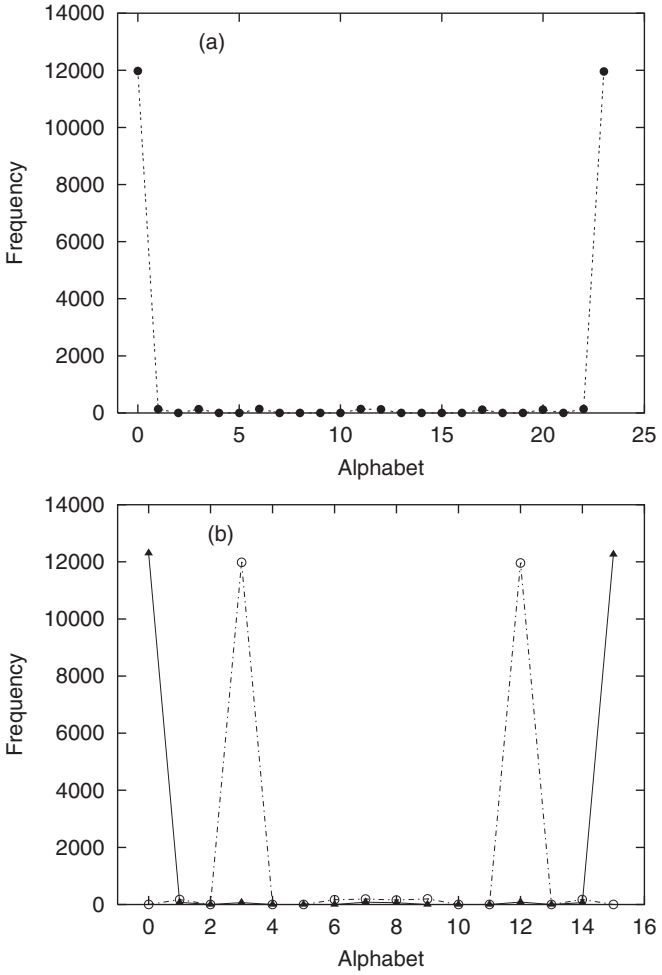

FIG. 1. Histograms of alphabets for the time series of the variable x of the Lorenz model. $T = 0.01$ ($k = 1$) and $D = 4$. (a) PE and (b) SEG (closed triangles) and SEL (open circles).

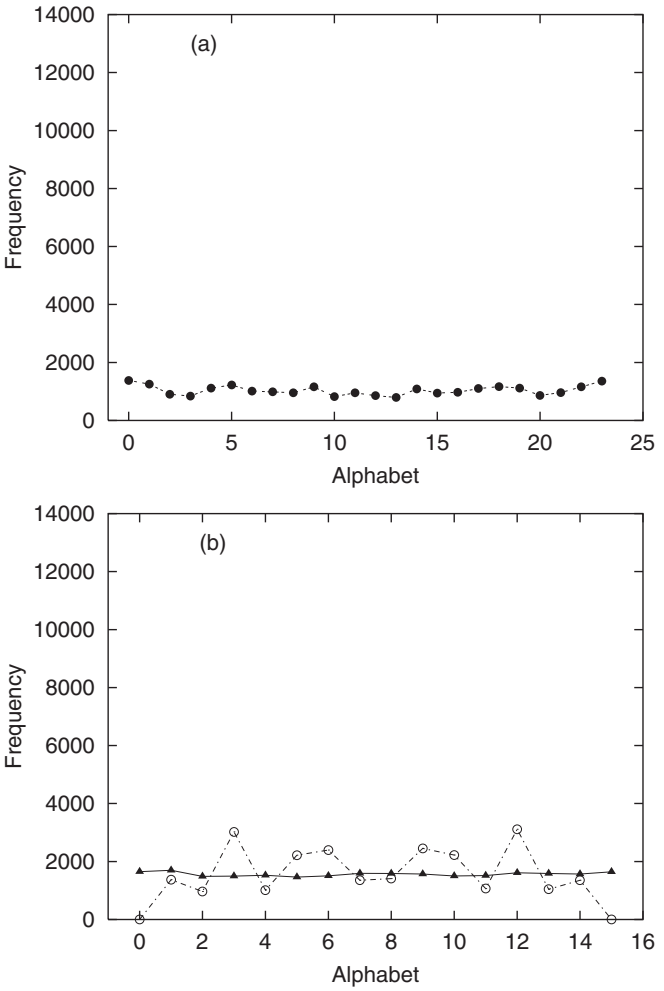

FIG. 2. Histograms of alphabets for the time series of the variable x of the Lorenz model. $T = 3$ ($k = 300$) and $D = 4$. (a) PE and (b) SEG (closed triangles) and SEL (open circles).

be interpreted to represent the sum of positive Lyapunov exponents, i.e., the KS entropy. The simplest form of f is $\beta = c\lambda$, where c is a positive constant. This holds if there is a linear correlation between α and λ, which leads to

$$c = \frac{\alpha}{\lambda}\frac{1}{h(0)[1-h(0)]}. \tag{8}$$

The validity of this idea is examined through our numerical experiments in the following section.

III. NUMERICAL ANALYSIS

A. Numerical time series

We conducted numerical experiments on estimating $h(0)$ and α for well-known dynamical models of chaotic flows published in Ref. [19], in which the mathematical forms of the models and their Lyapunov spectra were shown. In this study, D is set to 4. We numerically integrated the dynamical models using the fourth-order Runge-Kutta method with a time width Δt of 1×10^{-2} (1×10^{-4} only for the Hénon-Heiles system in Table I). The bifurcation parameters as well as the initial conditions were the same as those given in Ref. [19]. For all the dynamical models shown in Table I, the first 10^4 data points were discarded to eliminate the transient part depending on the initial conditions. We thus obtained numerical time series consisting of 10^5 data points (10^6 data points only for the Hénon-Heiles system) at sampling time intervals of $T = k \times \Delta t$ with $k = 1$, 2, 3, 4, 5, 10, 30, 50, 100, and 300. Estimates of $h(0)$ and α were obtained by applying least-mean-square fitting to $h(T)$ for $\Delta t \leqslant T \leqslant 5\Delta t$ on the basis of Eq. (4).

Table I summarizes our numerical results, where estimates of α, $h(0)$, and the correlation coefficient of the linear fitting as well as the largest Lyapunov exponent cited from Ref. [19] are shown for various chaotic models. The estimates of $h(0)$ are about 0.22 for PE and 0.25 for SEG and SEL, as have been theoretically predicted. As typical results, Figs. 1(a) and 1(b) show the histogram of the 24 alphabets for PE and those of the 16 alphabets for SEG and SEL, respectively, for the time series of the variable x of the Lorenz model with $T = \Delta t$. Similar results for $T = 300\Delta t$ are shown in Figs. 2(a) and 2(b). In Fig. 1(a), a pair of large peaks appear at the alphabets "1234" and "4321." In Fig. 1(b), a pair of large peaks appear at "0000" and "1111" for SEG and at "0011" and "1100" for SEL. In Figs. 1(b) and 2(b), "0000" and "1111" for SEL are missing.

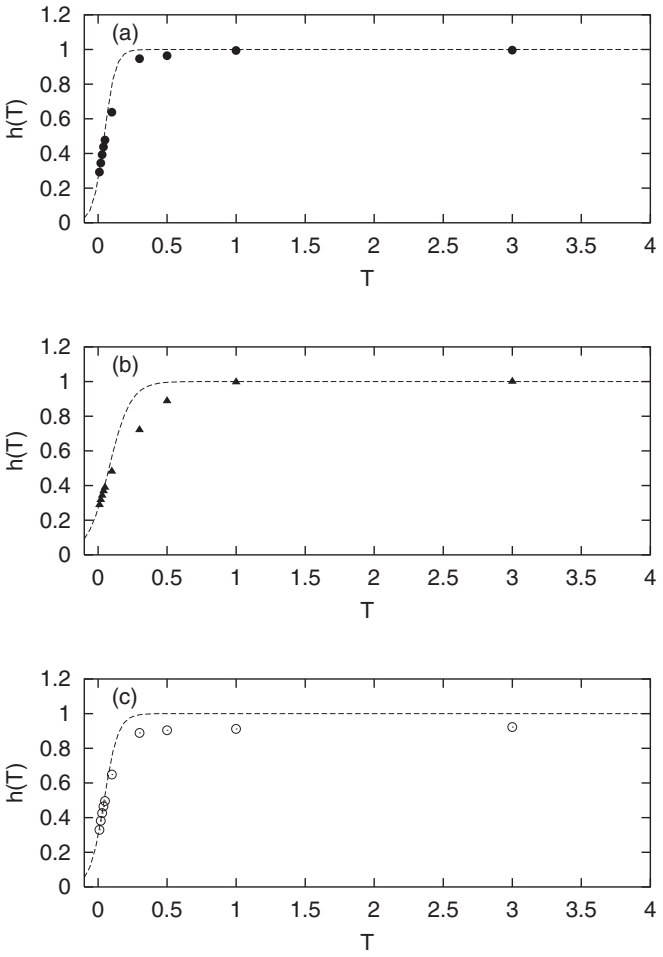

FIG. 3. Estimates of h as a function of T for the time series of the variable x of the Lorenz model. $D = 4$. (a) PE, (b) SEG, and (c) SEL. Dashed curves indicate the approximate functions defined by Eqs. (5) and (8), where the coefficient c was determined using the estimates of α, λ, and $h(0)$. The largest Lyapunov exponent λ is cited from Ref. [19].

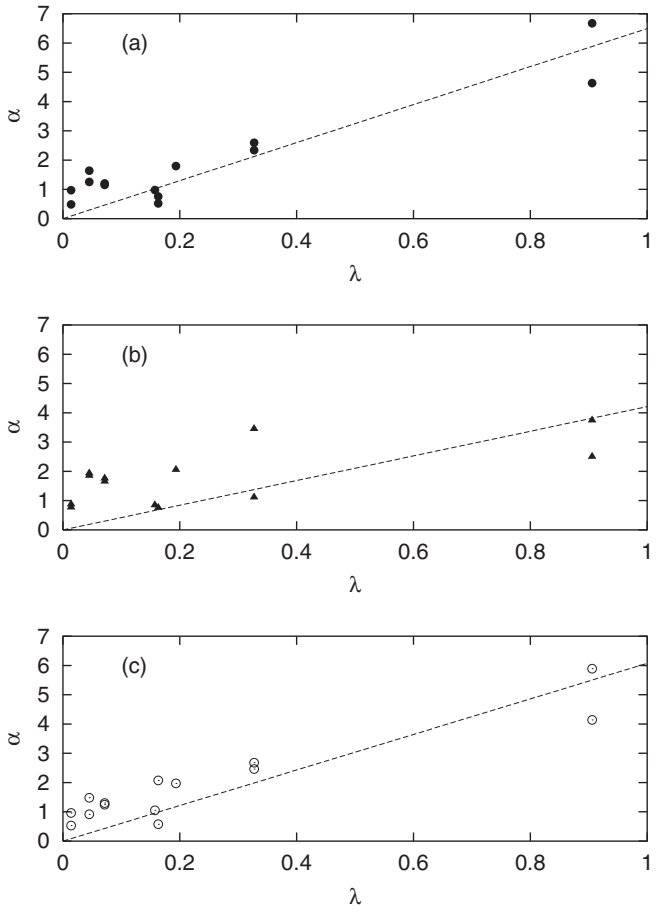

FIG. 4. Plots of α versus the largest Lyapunov exponent λ for (a) PE, (b) SEG, and (c) SEL.

Figures 3(a)–3(c) show estimates of $h(T)$ for the time series of the variable x of the Lorenz model for PE, SEG, and SEL, respectively, where the approximate curves of $h(T)$ defined by Eqs. (5) and (8) are also depicted using the estimates of α and $h(0)$ with the largest Lyapunov exponent λ published in Ref. [19]. The approximate curves appear to reproduce the overall features of $h(T)$.

Figures 4(a)–4(c) show the plots of α as functions of λ summarized in Table I for PE, SEG, and SEL, respectively, where linear lines determined by least-mean-square error fitting represent $\alpha = ch(0)[1 - h(0)]\lambda$ defined by Eq. (8). The linear correlation between α and λ is summarized in Table II. For PE and SEL, there are high linear correlations between α and λ, which is consistent with our assumption underlying Eq. (8).

To clarify the effect of the choice of D, the dependencies of α and $h(0)$ on D were examined through numerical experiments for the time series of the variables x and y of the Lorenz equations under the settings of $D = 5$ and 6. Other parameters and conditions were the same as those of the Lorenz equations shown in Table I. The results are summarized in Table III . As mentioned in Sec. II, our theoretical prediction regarding $h(0)$ is $1/D = 0.2$ and approximately 0.1667 for SEG and SEL and $1/\log_2 D! \approx 0.1448$ and 0.1054 for PE when $D = 5$ and 6, respectively. Notice that for PE the total number of alphabets amounts to $D! = 720$, much larger than $2^D = 64$, when $D = 6$. When $D = 5$, PE, and SEG reproduce the theoretical predictions regarding $h(0)$ as well as estimates of α similar to those shown in Table I. On the other hand, SEL yields different estimates. This is due to the ambiguity in defining the alphabets corresponding to $h(0)$, as mentioned in Sec. II. The ambiguity vanishes when $D = 6$. Figures 5(a) and 5(b) show histograms of the alphabets for SEG and SEL at $T = 0.01$ with $D = 5$ and 6, respectively. In Fig. 5(a), for SEL, there are four major peaks, which reflects the ambiguity

TABLE II. Estimates of α/λ and the correlation coefficient of the λ versus α plot, calculated from PE, SEG, and SEL for the chaotic models in Table I.

Entropy	α/λ	Correlation coefficient
PE	6.4937	0.9361
SEG	4.2117	0.6686
SEL	6.0731	0.9357

TABLE III. Estimates of α, $h(0)$, and the correlation coefficient of the linear fitting, calculated from PE, SEG, and SEL for the numerical time series of the variables x and y of the Lorenz equations. $D = 5$ and 6.

D	Model and variable	Entropy	α s^{-1}	$h(0)$	Correlation coefficient
5	Lorenz, x	PE	4.7339	0.1760	0.9971
		SEG	2.6588	0.2180	0.9984
		SEL	2.1449	0.4043	0.9998
5	Lorenz y	PE	7.1011	0.1895	0.9973
		SEG	3.9923	0.2292	0.9973
		SEL	3.7774	0.3984	0.9983
6	Lorenz, x	PE	4.7532	0.1338	0.9979
		SEG	2.8362	0.1826	0.9984
		SEL	6.0847	0.2293	0.9941
6	Lorenz y	PE	7.0843	0.1518	0.9965
		SEG	4.1516	0.1966	0.9965
		SEL	5.8294	0.2950	0.9829

induced by setting D to an odd integer. In contrast, there are two major peaks in Fig. 5(b).

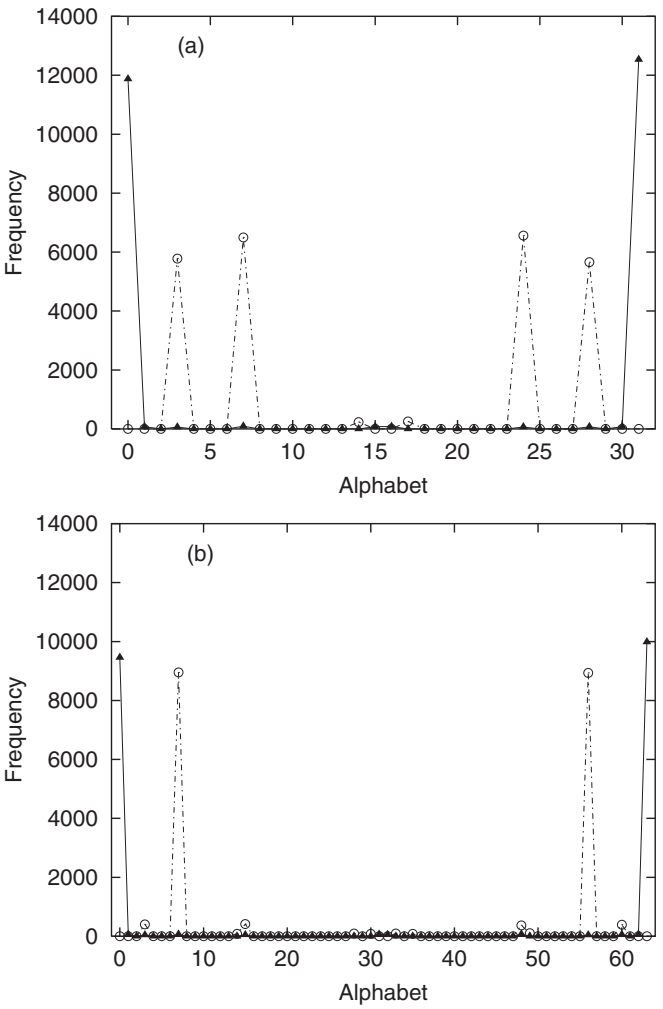

FIG. 5. Histograms of alphabets for the time series of the variable x of the Lorenz model for SEG (closed triangles) and SEL (open circles) at $T = 0.01$. (a) $D = 5$ and (b) $D = 6$.

B. Experimental time series

We next conducted numerical analysis of actually observed data: a time series of the flame front location of an unstable swirling premixed flame [20] and a time series of buoyancy-induced flame oscillations under a swirling flow [21]. In References [20] and [21], chaotic dynamical behavior was found to appear in both dynamical systems using other methods of time series analysis.

Figure 6 shows a time series of the flame front location of a swirling premixed flame with a bulk flow velocity of $u_0 = 1.6$ m/s observed with a time resolution of 10^{-3} s. For details of the experimental method, see Ref. [20]. The time series consists of 9900 data points. We estimated α and $h(0)$ by the linear fitting of $h(T)$ at $T = 0.001$, 0.002, 0.003, 0.004, and 0.005 s for PE, SEG, and SEL with $D = 4$. The estimates are summarized in Table IV and Figs. 7(a)–7(c) for PE, SEG,

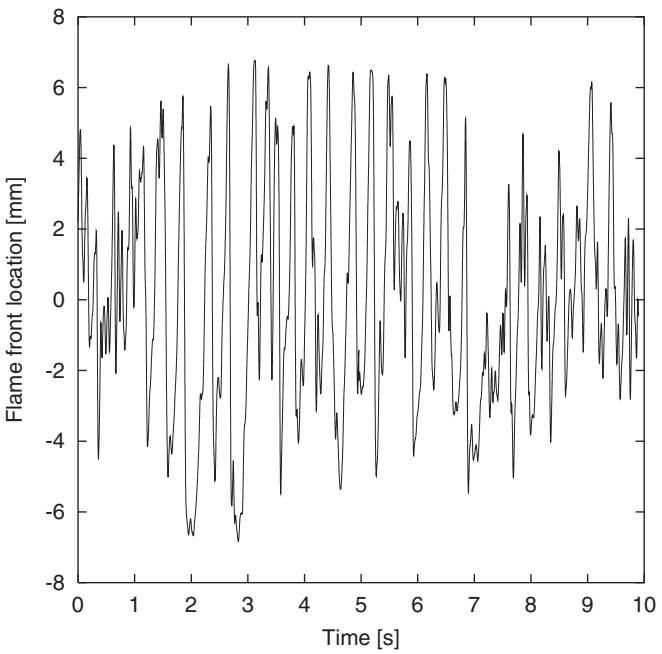

FIG. 6. Flame front location of an unstable swirling premixed flame as a function of time [20].

TABLE IV. Estimates of α, $h(0)$, and the correlation coefficient of the linear fitting, calculated from PE, SEG, and SEL for the experimental time series shown in Fig. 6.

Entropy	α s^{-1}	$h(0)$	Correlation coefficient
PE	62.43	0.1578	0.9989
SEG	30.48	0.2750	0.9874
SEL	35.01	0.3371	0.9960

and SEL, respectively, where the approximate curves of $h(T)$ defined by Eqs. (5) and (8) are depicted using the estimates of α and $h(0)$. For SEG and SEL, the approximate curves appear to better reproduce the overall features of $h(T)$.

We also estimated the largest Lyapunov exponent as a function of the embedding dimension using the algorithm of Rosenstein *et al.* [3]. The results are shown in Fig. 8. In Ref. [20], the degree of visible determinism was estimated as a function of the embedding dimension using the algorithm developed by Wayland *et al.* [22], from which the minimal embedding dimension was inferred to be 10. The largest Lyapunov exponent takes a value of 11.19 s^{-1} with a correlation coefficient of 0.9935 when the embedding dimension is 10.

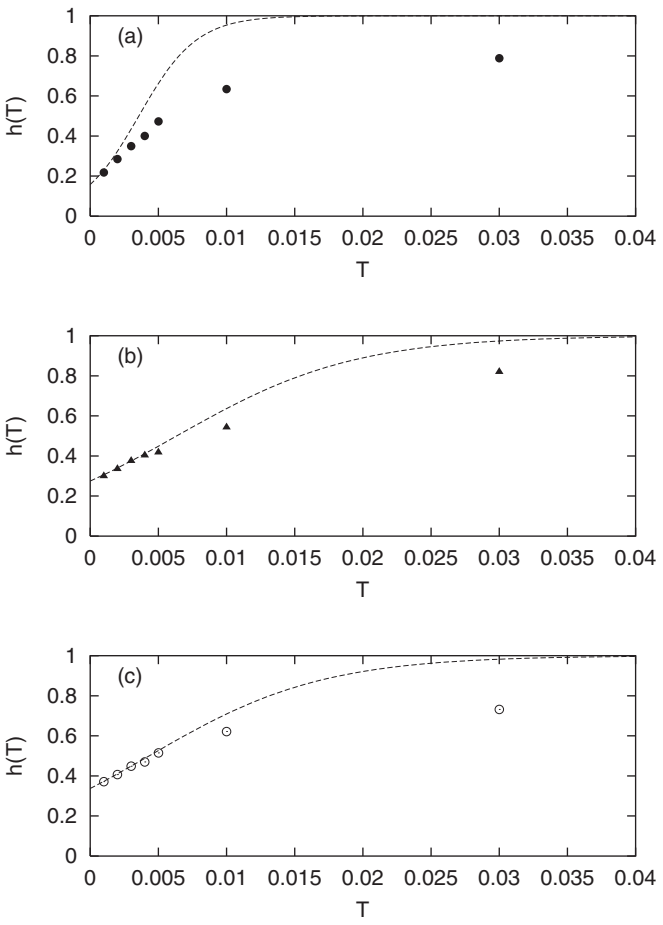

FIG. 7. Estimates of h as a function of T for the time series of the flame front location of an unstable swirling premixed flame. $D = 4$. (a) PE, (b) SEG, and (c) SEL. Dashed curves indicate the approximate functions defined by Eqs. (5) and (8).

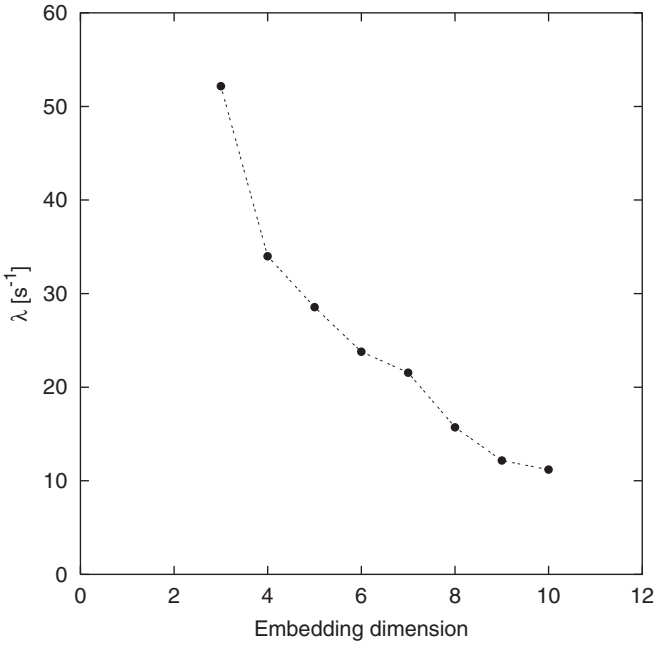

FIG. 8. Largest Lyapunov exponent λ as a function of the embedding dimension for the flame front location of an unstable swirling premixed flame.

Hence, $\alpha/\lambda = 5.579$, 2.724, and 3.129 for PE, SEG, and SEL, respectively. These values are of the same order as those shown in Table II, particularly for PE, despite noise contamination of the observed time series.

Figure 9 shows the flame front location of buoyancy-induced flame oscillations as a function of time, observed with a time resolution of 10^{-3} s, for a swirling flow with a rotational Reynolds number of $Re_r = 549$ and a swirl number

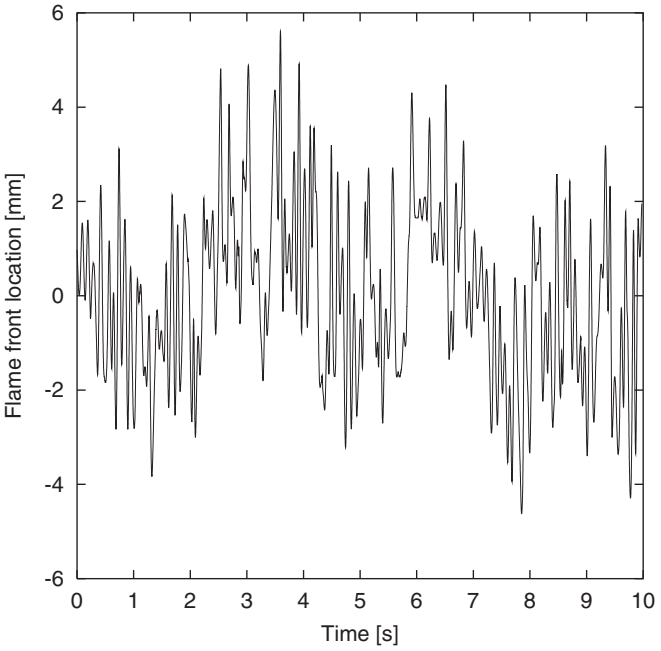

FIG. 9. Flame front location of buoyancy-induced flame oscillations as a function of time [21].

TABLE V. Estimates of α, $h(0)$, and the correlation coefficient of the linear fitting, calculated from PE, SEG, and SEL for the experimental time series shown in Fig. 9.

Entropy	α s^{-1}	$h(0)$	Correlation coefficient
PE	57.48	0.1599	0.9965
SEG	33.32	0.2949	0.9581
SEL	28.46	0.3699	0.9738

of $S = 2.4$. Details of the experimental method were given in Ref. [21]. The time series consists of 9980 data points. α and $h(0)$ were estimated by the linear fitting of $h(T)$ at $T = 0.001$, 0.002, 0.003, 0.004, and 0.005 s with $D = 4$ for PE, SEG, and SEL. The results are summarized in Table V and Figs. 10(a)–10(c) for PE, SEG, and SEL, respectively, where the approximate curves of $h(T)$ defined by Eqs. (5) and (8) are also depicted. Similarly to Figs. 6(a)– 6(c), for SEG and SEL, the approximate curves appear to better reproduce the overall features of $h(T)$.

The largest Lyapunov exponent was estimated as a function of the embedding dimension using the algorithm of Rosenstein *et al.* The results are shown in Fig. 11 . We also estimated the degree of visible determinism as a function of the embedding dimension in terms of the translation error of neighboring trajectories in phase space using the diagnostic algorithm of Wayland *et al.* in much the same way as in Ref. [20]. The results (data not shown) indicated that the translation error was 0.0411 at an embedding dimension of 10, which implies that the determinism underlying the time series is clearly visible when the embedding dimension is set to 10. At the embedding dimension of 10, $\lambda = 11.25$ s^{-1} with a correlation coefficient of 0.9797. Hence, $\alpha/\lambda = 5.107$, 2.961, and 2.529 for PE, SEG, and SEL, respectively, exhibiting a similar tendency to the time series shown in Fig. 6.

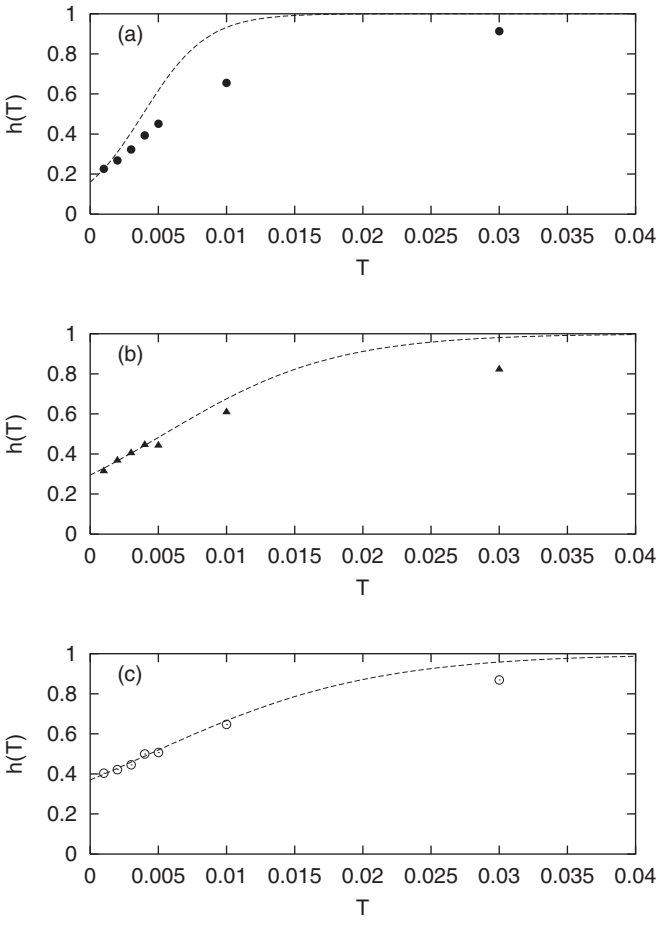

FIG. 10. Estimates of h as a function of T for the time series of the flame front location of buoyancy-induced flame oscillations. $D = 4$. (a) PE, (b) SEG, and (c) SEL. Dashed curves indicate the approximate functions defined by Eqs. (5) and (8).

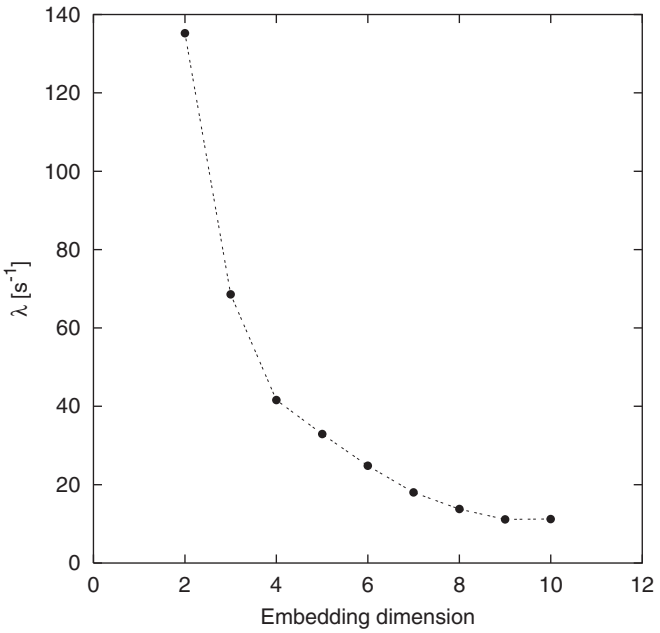

FIG. 11. Largest Lyapunov exponent λ as a function of the embedding dimension for the flame front location of buoyancy-induced flame oscillations.

IV. DISCUSSION

The underlying dynamics of the numerical data analyzed in Sec. III A are well-known systems of nonlinear ordinary differential equations that represent chaotic flows, each with a single positive Lyapunov exponent. For these numerical time series, our results indicate that there is a linear correlation between α and the largest Lyapunov exponent, especially for PE and SEL. The estimated histograms for the minimum sampling time interval, i.e., $T = 0.01$ ($T = 0.0001$ only for the Hénon-Heiles system), are consistent with our assumption that $h(0)$ corresponds to the limit of continuous measurement of a time series, as has been shown in Figs. 1(a) and 1(b). The estimated values of $h(0)$ are also consistent with our predictions of $h(0) = 1/\log_2(D!)$ for PE and $1/D$ for SEG and SEL when D is set to an even integer. The results shown in Table III and Figs. 5(a) and 5(b) indicate that D should be set to an even integer to avoid the ambiguity in defining the alphabets appearing in the limit of $T \to 0$ when using SEL. For PE and SEL, the coarse-graining of the time series into a sequence of alphabets was performed using local

rank scores and local thresholds, respectively, while for SEG the coarse-graining was performed over all segments of the series using a single global threshold. The difference between the local methods and the global method for generating alphabets is considered to result in the different estimates of α/λ.

In Figs. 3(a)–3(c), the approximate curves reproduce the overall features of $h(T)$. This implies that the entropy h as a function of time is subject to the logistic equation of the form

$$\frac{dh}{dt} = c\lambda h(1-h), \tag{9}$$

which is a well-known mathematical model of population dynamics. By integrating Eq. (9) from $t = 0$ to the sampling time T, we obtain Eq. (5) with $\beta = c\lambda$.

For the experimental time series shown in Figs. 6 and 9, PE yields estimated values of α/λ close to that estimated for the numerical time series shown in Table II, whereas SEG and SEL provide estimates smaller than those shown in Table II. For $h(0)$, only SEG approximately reproduces our theoretical prediction of $h(0) = 1/D$. These discrepancies in α/λ and $h(0)$ may be due to noise contamination of the experimental data as well as the estimation errors of the largest Lyapunov exponent caused by the algorithm of Rosenstein *et al.* In fact, SEG is the least sensitive to noise contamination of a time series owing to the use of a single global threshold to binarize the time series. Instead, the coarse-graining of the time series for SEG is of lower resolution and less sensitive to observational noise than that for PE and SEL, which may result in estimates of $h(0)$ close to $1/D$.

In existing methods for estimating the largest Lyapunov exponent from experimental time series such as the Kantz algorithm and that of Rosenstein *et al.*, wherein the distance between neighboring trajectories is measured as a function of time, the embedding dimension must be sufficiently large to exclude false neighboring trajectories. However, as the embedding dimension increases, the distance often tends to oscillate with time and consequently it becomes difficult to give a reliable estimation of the Lyapunov exponent [23]. In contrast, our method uses the parameter D as the number of contiguous data points in each segment of a time series to determine the total number of alphabets, not as the embedding dimension used to reconstruct the phase space. Hence, our method incurs neither the risk of false neighboring trajectories in choosing D nor unreliability in the estimated distance between trajectories. However, the total number of alphabets exponentially increases with D, meaning that a long time series is necessary to avoid a biased histogram of the alphabets when D is large. This problem is more serious in the case of PE since the total number of alphabets is $D!$ and much larger than 2^D. In this sense, SEG and SEL should yield unbiased estimates of α and λ when handling a short time series.

When treating experimental chaotic flows with a single positive Lyapunov exponent, our method is more robust and tractable than those for estimating the largest Lyapunov exponent, as has been demonstrated in the previous section. However, when handling experimental chaotic flows with multiple positive Lyapunov exponents, we must reinterpret what λ in Eq. (8) corresponds to. In this situation, λ should be interpreted as the sum of positive Lyapunov exponents. Then, α is a surrogate for the KS entropy: $\alpha \propto \sum_{i,\lambda_i>0} \lambda_i$.

Let us consider a time series representing a stochastic process having many degrees of freedom. In such a case, the dynamical system appears to have many $\lambda_i > 0$, and hence $\lambda \to \infty$. Consequently, $h(T)$ takes a value of unity regardless of T and $h(0)$ may not be well defined according to Eq. (8). Thus, stochastic processes can be discriminated from chaos by examining $h(T)$ at a sufficiently small value of T.

In this study, we have focused on the dynamical behavior of chaotic flows, which are expressed as ordinary differential equations with respect to time. One might wonder whether the proposed method is applicable to time series generated by chaotic maps such as the logistic map and the tent map. We think that the proposed method is generally inapplicable to times series generated by chaotic maps (unless one operation of a chaotic map corresponds to a sufficiently short sampling time interval of the corresponding chaotic flow) because $h(T)$ cannot be well defined in the limit of $T \to 0$, i.e., in the limit of continuous measurement of the time series.

V. CONCLUSIONS

We have proposed a mathematical method for assessing the degree of dynamical instability on the basis of the information entropy of symbolic time series. We have shown three procedures for transforming a time series into the corresponding symbolic sequences and subsequently estimating the information entropies, i.e., PE, SEG, and SEL, as functions of the sampling time interval of the time series from the histograms of the alphabets generated from the symbolic sequences. By linearizing the information entropy with respect to the sampling time interval, the gradient α and intersect $h(0)$ are calculated. We have shown that there is a linear correlation between α and the largest Lyapunov exponent λ in the case of a single positive Lyapunov exponent. In the case of multiple positive Lyapunov exponents, λ may be reinterpreted as the KS entropy. Thus, α can be a surrogate invariant measure for the largest Lyapunov exponent or the KS entropy. Since our method does not consider the distance between neighboring trajectories in phase space, it is robust to noise contamination of experimental time series.

Open questions are the existence of a universal constant between α and λ and the capability of the proposed method for discriminating stochastic processes from chaos. For the latter question, it is worth investigating the effect of the present method on surrogate symbolic dynamics generated under a variety of null hypotheses concerning the statistical properties of a given time series.

ACKNOWLEDGMENTS

We thank Dr. K. Cho for technical support. This study was partly supported by JSPS KAKENHI Grant No. JP15K00353.

[1] J.-P. Eckmann and D. Ruelle, Ergodic theory of chaos and strange attractors, Rev. Mod. Phys. **57**, 617 (1985).
[2] M. Sano and Y. Sawada, Measurement of the Lyapunov Spectrum from a Chaotic Time Series, Phys. Rev. Lett. **55**, 1082 (1985).
[3] M. T. Rosenstein, J. J. Collins, and C. J. De Luca, A practical method for calculating largest Lyapunov exponents from small data sets, Physica D **65**, 117 (1993).
[4] H. Kantz, A robust method to estimate the maximal Lyapunov exponent of a time series, Phys. Lett. A **185**, 77 (1994).
[5] C. E. Shannon, Communication theory of secrecy systems, Bell Syst. Tech. J. **28**, 656 (1949).
[6] A. M. Fraser and H. L. Swinney, Independent coordinates for strange attractors from mutual information, Phys. Rev. A **33**, 1134 (1986).
[7] A. M. Fraser, Information and entropy in strange attractors, IEEE Trans. Inf. Theory **35**, 245 (1989).
[8] M. Costa, A. L. Goldberger, and C.-K. Peng, Multiscale Entropy Analysis of Complex Physiologic Time Series, Phys. Rev. Lett. **89**, 068102 (2002).
[9] C. Bandt and B. Pompe, Permutation Entropy: A Natural Complexity Measure for Time Series, Phys. Rev. Lett. **88**, 174102 (2002).
[10] C. Bandt, G. Keller, and B. Pompe, Entropy of interval maps via permutations, Nonlinearity **15**, 1595 (2002).
[11] J. M. Amigó, M. B. Kennel, and L. Kocarev, The permutation entropy rate equals the metric entropy rate for ergodic information sources and ergodic dynamical systems, Physica D **210**, 77 (2005).
[12] L. Zunino, M. C. Soriano, I. Fisher, O. A. Rosso, and C. R. Mirasso, Permutation-information-theory approach to unveil delay dynamics from time-series analysis, Phys. Rev. E **82**, 046212 (2010).
[13] C. W. Kulp and S. Smith, Characterization of noisy symbolic time series, Phys. Rev. E **83**, 026201 (2011).
[14] L. Zunino, M. C. Soriano, and O. A. Rosso, Distinguishing chaotic and stochastic dynamics from time series by using a multiscale symbolic approach, Phys. Rev. E **86**, 046210 (2012).
[15] C. W. Kulp and L. Zunino, Discriminating chaotic and stochastic dynamics through the permutation spectrum test, Chaos **24**, 033116 (2014).
[16] A. Politi, Quantifying the Dynamical Complexity of Chaotic Time Series, Phys. Rev. Lett. **118**, 144101 (2017).
[17] M. Weilenmann, L. Kraemer, P. Faist, and R. Renner, Axiomatic Relation Between Thermodynamic and Information-Theoretic Entropies, Phys. Rev. Lett. **117**, 260601 (2016).
[18] C. Bian, C. Qin, Q. D. Y. Ma, and Q. Shen, Modified permutation-entropy analysis of heartbeat dynamics, Phys. Rev. E **85**, 021906 (2012).
[19] J. C. Sprott, *Chaos and Time-Series Analysis* (Oxford University Press, Oxford, 2003), pp. 428–440.
[20] H. Gotoda, T. Miyano, and I. G. Shepherd, Dynamic properties of unstable motion of swirling premixed flames generated by a change in gravitational orientation, Phys. Rev. E **81**, 026211 (2010).
[21] H. Gotoda, Y. Asano, K. H. Chuah, and G. Kushida, Nonlinear analysis on dynamic behavior of buoyancy-induced flame oscillation under swirling flow, Int. J. Heat Mass Transf. **52**, 5423 (2009).
[22] R. Wayland, D. Bromley, D. Pickett, and A. Passamante, Recognizing Determinism in a Time Series, Phys. Rev. Lett. **70**, 580 (1993).
[23] H. Kantz and T. Schreiber, *Nonlinear Time Series Analysis* (Cambridge University Press, Cambridge, 1997), pp. 66–67.